Available online at www.sciencedirect.com

ScienceDirect

Geochimica et Cosmochimica Acta 174 (2016) 335–344

Geochimica et Cosmochimica Acta

www.elsevier.com/locate/gca

Calcium isotopic composition of mantle xenoliths and minerals from Eastern China

Jin-Ting Kang [a,b], Hong-Li Zhu [b,c], Yu-Fei Liu [b,c], Fang Liu [b,c], Fei Wu [a], Yan-Tao Hao [a], Xia-Chen Zhi [a], Zhao-Feng Zhang [b,*], Fang Huang [a,*]

[a] CAS Key Laboratory of Crust-Mantle Materials and Environments, School of Earth and Space Sciences, University of Science and Technology of China, Hefei 230026, China

[b] State Key Laboratory of Isotope Geochemistry, Guangzhou Institute of Geochemistry, The Chinese Academy of Sciences, Guangzhou 510640, China

[c] University of Chinese Academy of Sciences, Beijing 100049, China

Received 2 May 2015; accepted in revised form 26 November 2015; Available online 5 December 2015

Abstract

This study presents calcium isotope data for co-existing clinopyroxenes (cpx), orthopyroxenes (opx), and olivine (ol) in mantle xenoliths to investigate Ca isotopic fractionation in the upper mantle. $\delta^{44/40}Ca$ ($\delta^{44/40}Ca$ (‰) = $(^{44}Ca/^{40}Ca)_{SAMPLE}/(^{44}Ca/^{40}Ca)_{SRM915a} - 1$) in opx varies from 0.95 ± 0.05‰ to 1.82 ± 0.01‰ and cpx from 0.71 ± 0.06‰ to 1.03 ± 0.12‰ (2se). $\delta^{44/40}Ca$ in ol (P-15) is 1.16 ± 0.08‰, identical to $\delta^{44/40}Ca$ of the co-existing opx (1.12 ± 0.09‰, 2se). The $\Delta^{44/40}Ca_{opx-cpx}$ ($\Delta^{44/40}Ca_{opx-cpx} = \delta^{44/40}Ca_{opx} - \delta^{44/40}Ca_{cpx}$) shows a large variation ranging from −0.01‰ to 1.11‰ and it dramatically increases with decreasing of Ca/Mg (atomic ratio) in opx. These observations may reflect the effect of opx composition on the inter-mineral equilibrium fractionation of Ca isotopes, consistent with the theoretical prediction by first-principles theory calculations (Feng et al., 2014). Furthermore, $\Delta^{44/40}Ca_{opx-cpx}$ decreases when temperature slightly increases from 1196 to 1267 K. However, the magnitude of such inter-mineral isotopic fractionation (1.12‰) is not consistent with the value calculated by the well-known correlation between inter-mineral isotope fractionation factors and $1/T^2$ (Urey, 1947). Instead, it may reflect the temperature control on crystal chemistry of opx (i.e., Ca content), which further affects $\Delta^{44/40}Ca_{opx-cpx}$. The calculated $\delta^{44/40}Ca$ of bulk peridotites and pyroxenites range from 0.76 ± 0.06‰ to 1.04 ± 0.12‰ (2se). Notably, $\delta^{44/40}Ca$ of bulk peridotites are positively correlated with CaO and negatively with MgO content. Such correlations can be explained by mixing between a fertile mantle end-member and a depleted one with low $\delta^{44/40}Ca$, indicating that Ca isotopes could be a useful tool in studying mantle evolution.

© 2015 Elsevier Ltd. All rights reserved.

1. INTRODUCTION

Ca is the fifth most abundant element in the Earth and one of the major rock-forming elements and also an essential nutrient in the marine and terrestrial biosphere. Ca has six stable isotopes (^{40}Ca, ^{42}Ca, ^{43}Ca, ^{44}Ca, ^{46}Ca, and ^{48}Ca) with the largest relative mass differences of stable isotopes ($\Delta m/m = 20\%$) in the periodic table except H and He. Due to advances in mass spectrometry technique, Ca isotopic variations have been documented in terrestrial samples including rocks and sediments, demonstrating significant fractionation associated with numerous geochemical processes. Therefore, Ca isotopes can be used as a meaningful tracer to constrain Ca transport in planetary accretion, mantle evolution (e.g., Simon and DePaolo,

* Corresponding authors.
E-mail addresses: zfzhang@gig.ac.cn (Z.-F. Zhang), fhuang@ustc.edu.cn (F. Huang).

http://dx.doi.org/10.1016/j.gca.2015.11.039
0016-7037/© 2015 Elsevier Ltd. All rights reserved.

2010; Huang et al., 2012; Valdes et al., 2014), ocean water cycling (e.g., Zhu and Macdougall, 1998; De La Rocha and DePaolo, 2000; Hippler et al., 2003; Fantle and DePaolo, 2007; Farkaš et al., 2007; Griffith et al., 2008), and biochemical processes (e.g., Morgan et al., 2012).

Recent observations have shown considerable Ca isotopic fractionation in both mineral and bulk rock scales in the upper mantle. Huang et al. (2010) observed large offsets in $\Delta^{44/40}$Ca (up to 0.75‰) between opx and cpx from peridotite xenoliths. Such large inter-mineral Ca isotopic fractionation could be attributed to the differences in Ca–O bond length between cpx and opx. Based on first-principles calculation results, Feng et al. (2014) proposed that the inter-mineral Ca isotopic fractionation between cpx and opx may reflect the effect of opx compositions on equilibrium isotopic fractionation. A negative correlation between Ca/Mg (atomic ratio) of opx and $\Delta^{44/40}Ca_{opx-cpx}$ was predicted in Feng et al. (2014). When Ca/Mg of opx is below 0.01, there is significant Ca isotopic fractionation between opx and cpx with $\Delta^{44/40}Ca_{opx-cpx}$ up to 1–2‰.

$\delta^{44/40}$Ca of mantle peridotites show a variation from 0.96‰ to 1.15‰ in previous studies (Amini et al., 2009; Huang et al., 2010; Simon and DePaolo, 2010). Amini et al. (2009) observed that $\delta^{44/40}$Ca of ultramafic rocks was negatively correlated with CaO content but positively correlated with MgO content, suggesting that igneous processes could cause Ca isotopic fractionation in mantle rocks. A recent study on a series of mantle-derived igneous rocks including OIB, komatiites, carbonatites, and mantle xenoliths by Chen et al. (2014) revealed more Ca isotopic heterogeneity in mantle rocks. However, Ca isotope data for mineral pairs and bulk rocks are still rare, limiting our understanding of the mechanisms for Ca isotope fractionation at high temperatures.

Xenoliths are widely found in Cenozoic basalts in the North China Craton (NCC) and Yangtze Craton (YC) in Eastern China. Comparison of geochemical compositions of basalts from the NCC formed before 110 Ma with those after 110 Ma indicates that the post 110 Ma basalts have signatures of subducted oceanic crust (e.g., low δ^{26}Mg, high U/Pb and Th/Pb ratios) (e.g., Huang et al., 2007; Yang and Li, 2008; Zhang et al., 2009; Xu et al., 2010; Wang et al., 2011). Furthermore, major and trace element and Re–Os isotope data show that lithospheric mantle of Eastern China has experienced different degrees of melt extraction (Xia et al., 2004; Reisberg et al., 2005). F. Huang et al. (2011) also reported Mg and Fe isotope data for xenoliths from Lianshan, Eastern China, showing that mantle minerals are in isotopic equilibrium. Thus, these xenoliths provide a good opportunity to study Ca isotopic composition of mantle rocks and minerals, as well as the feedback of Ca isotopes to mantle evolution processes (e.g., melt extraction and carbonate metasomatism).

In this study, we measured ^{44}Ca/^{40}Ca of co-existing pyroxene pairs in mantle peridotite and pyroxenite xenoliths from Eastern China. In addition, although CaO content in ol (<0.05 wt.%) is much lower than that in cpx (~22 wt.%) and opx (~0.6 wt.%), we also measured an ol sample for more comprehensive understanding of Ca isotopic composition of mantle minerals. The aim of this study is to investigate the mechanism for Ca isotopic fractionation between mantle minerals and evaluate the effects of metasomatism and melt extraction on Ca isotopic composition of peridotites.

2. GEOLOGIC BACKGROUND AND SAMPLE DESCRIPTION

Eastern China consists of three parts: North China Craton (NCC), Yangtze Craton (YC) and Cathaysia Block. Samples in this study were collected from NCC and YC. The NCC is the largest and oldest craton in China, bounded by the Xing'an Mongolian orogenic belt on the north and the Qinling–Dabie–Sulu high-ultrahigh pressure metamorphic belt on the south and east (e.g., Jahn et al., 1987; Zhao et al., 2000; Kusky et al., 2001). The NCC consists of two Archean blocks separated by a 1.8 Ga Proterozoic orogenic belt (Zhao et al., 2000). The YC is mainly Proterozoic which may have experienced multi-stage reworking of Archean crustal materials as indicated by zircon U–Pb age and Hf isotope data (Zhang et al., 2006). A simplified map with sample sites are available in supplementary materials S-Fig. 1.

According to the studies on Ordovician diamond-bearing kimberlites and mantle xenoliths, a thick (200 km) cold lithosphere existed in the NCC in the Paleozoic (e.g., Griffin et al., 1998; Menzies and Xu, 1998). However, geophysical studies indicated that the lithosphere of the NCC is thin at present (Chen et al., 2008, 2009), suggesting lithospheric thinning of ~100 km since the Paleozoic. Another important geologic event was the continental collision between the NCC and the YC along the Qinling–Dabie–Sulu zone in the Triassic, which formed the eastern part of the central orogenic belt in China (supplementary material S-Fig. 1) (e.g., Li et al., 1993).

Eastern China experienced widespread Cenozoic basaltic volcanism, probably related to the further lithospheric thinning in the Cenozoic. The strata comprises interlayered tholeiitic and alkali basalts with OIB-like Sr–Nd–Pb isotopic signature and trace element patterns (e.g., Tang et al., 2006). The alkali basalts contain abundant mantle xenoliths including spinel peridotites, pyroxenites, and mafic to felsic granulites. Four spinel lherzolite (P-1, P-9, P-10, and P-15) and two pyroxenite (H-3 and H-16) xenoliths were collected from the Hannuoba area situated along the north margin of the NCC, and three spinel lherzolite xenoliths (LHLS-4, LHLS-6, and LHLS-10) were from the Lianshan area situated in the YC (S-Fig. 1). Previous studies indicated that all samples have experienced different degrees of partial melting (Xia et al., 2004; Reisberg et al., 2005; F. Huang et al., 2011). Samples selected in this study are fresh and coarse-grained without any visible alteration in minerals, avoiding possible Ca isotopic fractionation caused by low temperature secondary processes such as weathering and alteration. The mineral modes (Table 2) of Lianshan samples are from F. Huang et al. (2011) and the modes for Hannuoba samples (P-1, P-9, P-10, P-15, H-3, and H-16) were calculated from major element compositions of bulk rocks and minerals using the least-squares method (elemental data can be found in supplementary material S-Table 1).

3. ANALYTICAL METHODS

Major element compositions were determined by electron microprobe (JEOL, JXA-8230) at Hefei University of Technology. Analytical conditions included an accelerating voltage of 15 kV, a beam current of 20 nA, and a beam size of 3 μm. Analytical errors were calculated based on 3–6 analyses of different spots. The following standards were used: garnet (Al, Fe, and Mn), tremolite (Si and Mg), albite (Ca), jadeite (Na), biotite (K), spinel (Cr), and olivine (Ni). Major element compositions of minerals and bulk rocks are available in Supplementary materials S-Table1. Rare earth element (REE) compositions of whole rock are from Xia et al. (2004) and Reisberg et al. (2005) (see more details in S-Table 3 and S-Fig. 2).

Mineral separation was conducted under a binocular microscope by handpicking clear and fresh ol, cpx, opx, and spl (spinel). As emphasized by Huang et al. (2010), because carbonate is usually isotopically lighter than mantle minerals (Fantle and Tipper, 2014 and references there in), carbonate precipitated on mineral surfaces can bias the Ca isotopic ratios of silicate minerals. Thus, in order to remove any possible calcium carbonate ($CaCO_3$) on the mineral surfaces, handpicked minerals were cleaned in ~1–2 ml milli-Q water twice in an ultrasonic bath for 20 min and leached in 6 ml 1 N HCl overnight at room temperature, followed by rinsing with milli-Q water several times. Finally, they were powdered in an agate mortar. In order to investigate analytical bias caused by carbonate precipitation on mineral surfaces, a duplicated opx from P-1 was only processed with milli-Q water in an ultrasonic bath before dissolution.

The chemical purification procedure for Ca follows Zhang et al. (2013), Zhu et al. (2013, in press), and Liu et al. (2013). Briefly, about 1 mg cpx, 15 mg opx, or 50 mg ol were weighed into a 7 ml PFA beaker. After digestion using a mixture of concentrated HF and HNO_3 (3:1) in a 7 ml PFA beaker on hot plate at 110 °C for 2–3 days, the samples were dried down at 80 °C. An aliquot containing ~50 μg Ca was transferred into a pre-cleaned PFA beaker and mixed with a ^{42}Ca–^{43}Ca double spike. We used 1 ml cation exchange resin (Bio-Rad AG MP-50, 100–200 mesh) in HCl media to remove matrix elements from Ca. In order to obtain pure Ca solution, the same procedure needs to be processed twice. Ca yield for the total chemical procedure is greater than 99%. As Ca content of ol is usually lower than 0.05 wt.%, the amount of Ca in dissolved ol aliquot was decreased down to 10–20 μg Ca so that the cation resin column was not over-loaded by matrix elements.

Ca isotopic ratios were determined on a thermal ionization mass-spectrometer (Thermo Triton) in the State Key Laboratory of Isotope Geochemistry, Guangzhou Institute of Geochemistry (GIG), Chinese Academy of Sciences (CAS). A single-sequence cup configuration was adopted so that ^{40}Ca, ^{41}K, ^{42}Ca, ^{43}Ca, and ^{44}Ca ion beams could be simultaneously measured. Mass 41 was measured for ^{41}K to monitor interference from $^{40}K^+$ ($^{40}K/^{41}K = 1.7384 \times 10^{-3}$). We used an iterative algorithm for data reduction similar to the routine of Heuser et al. (2002) using an exponential law. All results are reported relative to NIST SRM 915a as $\delta^{44/40}Ca$.

The whole procedural blank was 30–50 ng for pyroxene measurements and 70 ng for ol, which is insignificant relative to the amount of Ca processed through the purification procedure. SRM 915a and seawater standard (IAPSO) were routinely measured to monitor instrumental stability and reproducibility. If the sample was measured for three or more times, the errors were reported as 2 standard errors of the mean (marked as 2se). If it was measured only once or twice, the error for $\delta^{44/40}Ca$ was set as 0.12‰ based on 2 standard deviations of our long-term standard analyses (Table 1). The long-term average $\delta^{44/40}Ca$ of SRM 915a and IAPSO seawater are -0.01 ± 0.02‰ ($n = 33$, 2se) and 1.83 ± 0.03‰ ($n = 17$, 2se), respectively (Table 1), consistent with previous studies (Skulan et al., 1997; Hippler et al., 2003; DePaolo, 2004). The analysis error is comparable with Huang et al. (2010) (0.03‰, 2se for IAPSO seawater; 0.02‰, 2se for SRM 915a) and Valdes et al. (2014) (0.02‰, 2se for SRM 915a). Three samples (H-16 opx, P-10 opx, and P-10 cpx) were replicated by digestion of separate mineral grain aliquots, all showing good reproducibility in Ca isotopic data (Table 1).

4. RESULTS

Ca isotopic compositions for cpx, opx, and ol from Hannuoba and Lianshan xenoliths are reported in Table 1 and Fig. 1. The $\delta^{44/40}Ca$ of cpx ranges from 0.71‰ to 1.03‰. This range is significantly larger than our analytical uncertainties (0.03‰ for 2se and 0.12‰ for 2sd, Table 2). Notably, $\delta^{44/40}Ca$ of opx shows a larger variation (0.95–1.82‰) than cpx (Table 1 and Fig. 1). $\delta^{44/40}Ca$ of ol from P-15 is 1.16 ± 0.08‰ (2se), consistent with the co-existing opx (1.12 ± 0.09‰), but heavier than the co-existing cpx (0.91 ± 0.04‰). The $\delta^{44/40}Ca$ of cpx from two pyroxenites (H-3 and H-16) are 0.82 ± 0.03‰ and 0.92 ± 0.05‰, respectively, while $\delta^{44/40}Ca$ of opx in H-3 and H-16 are 1.44 ± 0.10‰ and 1.05 ± 0.05‰, respectively (Table 1 and Fig. 1). Table 1 and Fig. 1 show that $\delta^{44/40}Ca$ of most opx in peridotites are significantly heavier than the co-existing cpx with $\Delta^{44/40}Ca_{opx-cpx}$ ranging from 0.16‰ to 1.11‰. This is consistent with the data reported in Huang et al. (2010) in the sense of direction of isotopic fractionation ($\Delta^{44/40}Ca_{opx-cpx} = 0.36$‰ and 0.75‰). Yet, $\delta^{44/40}Ca$ of two pyroxenes in P-10 are identical in analytical error (0.96 ± 0.04‰ v.s. 0.95 ± 0.05‰, cpx vs. opx) with $\Delta^{44/40}Ca_{opx-cpx}$ of −0.01‰. The $\delta^{44/40}Ca$ of the acid-leached P-1 opx is 1.77 ± 0.01‰, identical to the P-1 opx without acid-leaching (1.76 ± 0.12‰), indicating that carbonates on the mineral surface (if any) do not significantly affect the $\delta^{44/40}Ca$ of opx measured in this study. Furthermore, it also indicates that our HCl leaching process did not introduce any measurable Ca isotopic variation. Nonetheless, in order to avoid possible isotopic bias caused by surface carbonates, we leached all the samples before digestion.

Table 1
Ca isotopic composition of Hannuoba and Lianshan xenoliths and standards.

	Hannuoba lherzolite											
	Clinopyroxene				Orthopyroxene				Olivine			
	$\delta^{44/40}$Ca(‰)	2se[a]	2sd	n[b]	$\delta^{44/40}$Ca(‰)	2se[a]	2sd	n[b]	$\delta^{44/40}$Ca(‰)	2se[a]	2sd	n[b]
P-1 leached	0.77	0.03	0.05	3	1.77	0.01	0.02	3				
P-1 unleached					1.76	0.12	0.17	2				
P-1 mean					1.77	0.01	0.02	5				
P-9	0.71	0.06	0.10	3	1.82	0.01	0.02	3				
P-10	0.98	0.04	0.08	4	0.98	0.07	0.12	3				
P-10 repeated	0.95	0.06	0.12	4	0.92	0.05	0.09	3				
P-10 mean	0.96	0.04	0.11	8	0.95	0.05	0.12	6				
P-15	0.91	0.04	0.07	3	1.12	0.09	0.16	3	1.16	0.08	0.14	3
H-3	0.82	0.03	0.05	3	1.44	0.1	0.17	3				
H-16	0.92	0.05	0.11	5	1.08	0.09	0.16	3				
H-16 repeated					1.03	0.04	0.07	3				
H-16 mean					1.05	0.05	0.12	6				
Lianshan lherzolite												
LHLS-4	0.94	0.12	0.12	1	1.34	0.12	0.12	1				
LHLS-6	1.03	0.12	0.12	1	1.31	0.12	0.12	1				
LHLS-10	0.83	0.12	0.12	1	1.21	0.12	0.12	1				
Standards												
SRM 915a	−0.01	0.02	0.11	33								
IAPSO seawater	1.83	0.03	0.12	17								

[a] $2se = 2sd/\sqrt{n}$. If only once or twice analysis of the sample was available, the error of $\delta^{44/40}$Ca was set as 0.12‰ based on the long-term measurements of seawater, reflecting the external reproducibility of our analyses.
[b] n = number for replicate analyses.

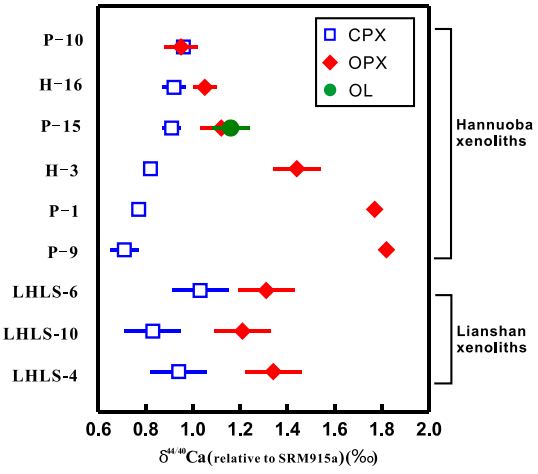

Fig. 1. Ca isotopic compositions of cpx, opx and ol in this study. The open symbols represent cpx and the solid symbols are opx and ol. The $\delta^{44/40}$Ca of cpx show a narrow range from 0.71‰ to 1.03‰, while Ca isotopic composition of opx is significantly heavier than cpx (0.95–1.82‰). $\delta^{44/40}$Ca of ol from P-15 is 1.16 ± 0.08‰, consistent with the co-existing opx in the direction of isotope fractionation. The error bars used 2se value from Table 1 and some are smaller than the symbols.

5. DISCUSSION

5.1. Equilibrium or disequilibrium isotope fractionation?

Before discussing the origin of Ca isotopic fractionation and the implications for mantle evolution, it is important to evaluate whether xenoliths in this study are in chemical equilibrium or not. Several lines of evidence indicate that chemical equilibrium has been achieved within these xenoliths on the scale of hand samples: (1) pyroxenes in peridotites (including both Hannuoba and Lianshan samples) are compositionally homogeneous (S-Table 1). Both opx and cpx display limited variations in Mg# (90.56–92.02 for cpx; 90.13–91.14 for opx), and Al_2O_3 (5.96–6.69 wt.% for cpx; 3.71–4.55 wt.% for opx); (2) Petrographic observations do not show obvious compositional zoning in minerals within these xenoliths; (3) Fe–Mg exchange factor between opx and cpx ranges from 0.87 to 1.00 (Table 2), close to the calibrated equilibrium value (1.09 ± 0.14) (Putirka, 2008); (4) Equilibrium temperature estimated by the two-pyroxene thermometers (Putirka, 2008) and Ca-in-orthopyroxene thermometers (Brey and Kohler, 1990) for each sample are identical within the error (i.e., ~50 °C) (Table 2). Hence, the Ca isotopic offset between opx and cpx should reflect equilibrium fractionation.

5.2. Compositional effect on inter-mineral Ca isotopic fractionation

Theoretical studies indicated that the bonding environment of elements dominate equilibrium inter-mineral isotopic fractionation, with stronger bonding favoring incorporation of heavy isotopes (e.g., Urey, 1947). Because the coordination number of Ca is 8 in cpx and 6 in opx and ol, heavy Ca isotopes should be preferentially enriched in opx and ol relative to cpx (Huang et al., 2010), which is generally consistent with our observations. However, a

Table 2
$\delta^{44/40}$Ca (‰), equilibrium temperature (K), mineral modes (%), and Ca–Mg contents (wt.%) of bulk rocks.

Sample	CaO	MgO	Mg#	T(P)	T(BK)	P (GPa)	K_D(Fe–Mg)	ol	cpx	opx	spl	$\delta^{44/40}$Ca	2se
P-1	2.36	40.82	91.7	1234	1194	1.02	0.87	65	12	21	2	0.81	0.03
P-9	1.79	41.72	91.1	1218	1196	1.04	0.89	70	9	20	1	0.76	0.06
P-10	2.66	40.88	91.6	1256	1273	1.14	1.00	67	15	17	1	0.96	0.04
P-15	2.76	38.86	91.4	1196	1239	1.14	0.94	53	15	30	2	0.92	0.04
H-3	14.97	18.94	87.2	1232	1204	1.11	0.85	0	32	68	0	0.93	0.03
H-16	2.00	29.42	89.3	1267	1292	1.13	1.00	0	8	92	0	0.83	0.05
LHLS4	2.78	40.76	90.1	1239	1250	0.96	0.94	62	13	25	1	0.96	0.12
LHLS6	3.21	39.25	89.7	1246	1252	1.09	0.91	60	15	23	2	0.85	0.12
LHLS10	3.51	37.83	89.6	1237	1238	1.18	0.95	54	16	28	2	1.04	0.12

Elemental compositions of Lianshan peridotites are from Reisberg et al. (2005) and Hannuoba samples are from Xia et al. (2004). Pressures were calculated using the two-pyroxene barometers in Putirka (2008). T (P) stands for temperatures calculated from two-pyroxene thermometry in Putirka (2008). And K_D(Fe–Mg) stands for the observed Fe–Mg exchange factor which should be near 1.09 ± 0.14 if elemental exchange equilibrium between two pyroxenes has been achieved (Putirka, 2008). T(BK) stands for temperatures calculated from Ca content in orthopyroxene thermometer using the method in Brey and Kohler (1990). Because cpx dominates Ca budget of the bulk rock, we used the analytical error of cpx measurements as the error of estimated $\delta^{44/40}$Ca in bulk rocks. Mineral modes of Hannuoba samples (P-1, P-9, P-10, P-15, H-3, and H-16) were calculated from major elements compositions of bulk rocks and minerals (ol, cpx, opx and spl) using the least-squares method. Elemental data can be found in supplementary material S-Table 1. Mineral modes of Lianshan samples are from F. Huang et al. (2011).

question that now arises is why $\Delta^{44/40}Ca_{opx-cpx}$ in xenoliths from Eastern China span a large range from −0.01‰ to 1.11‰.

Equilibrium Ca isotopic fractionation between cpx and opx can be approximated as:

$$\Delta^{44/40}Ca_{opx-cpx} = \delta^{44/40}Ca_{opx} - \delta^{44/40}Ca_{cpx} \cong 10^3 \ln \alpha^{44/40}_{opx-cpx} = \frac{10^3}{24}\left(\frac{h}{k_b T}\right)^2 \left(\frac{1}{m_{40}} - \frac{1}{m_{44}}\right)\left[\frac{K_{f,opx}}{4\pi^2} - \frac{K_{f,cpx}}{4\pi^2}\right]$$

where $\alpha^{44/40}_{opx-cpx}$ is the equilibrium Ca isotopic fractionation factor between cpx and opx; m_{40} and m_{44} are the atomic masses of ^{40}Ca and ^{44}Ca, respectively; k_b is Boltzmann's constant; h is Plank's constant; T is temperature in kelvin; $K_{f,opx}$ and $K_{f,cpx}$ are the average force constants for opx and cpx, respectively (e.g., Urey, 1947; Young et al., 2015; Macris et al., 2015). This equation indicates that Ca isotopic fractionation between cpx and opx is a linear function of $1/T^2$ if mass difference between isotopes and the differences in force constants are unchangeable. However, the temperature variation and mass differences denoted by $\sim\left(\frac{1}{T^2}\right)\left(\frac{1}{m_{40}} - \frac{1}{m_{44}}\right)$ cannot explain such large inter-mineral fractionation observed in our study. Varying temperature from 1196 K to 1267 K can only change $\Delta^{44/40}Ca_{opx-cpx}$ by 0.13‰. Alternatively, based on first-principles calculations of Feng et al. (2014), force constants of Ca isotopes in opx are controlled by the proportions of Ca substitution in the M1 site in opx. Particularly, Feng et al. (2014) indicated that $\Delta^{44/40}Ca_{opx-cpx}$ strongly depends on the Ca content of opx when Ca/Mg (atomic ratio) is lower than 0.067. As shown in Fig. 2, $\Delta^{44/40}Ca_{opx-cpx}$ increases dramatically with decreasing Ca/Mg of opx in peridotites and pyroxenites from Hannuoba and Lianshan, consistent with the trend predicted by the first-principles method in Feng et al. (2014). Therefore, the compositional control of opx is the most reasonable explanation for the inter-mineral Ca isotopic variation.

It is worth noting that the observed cpx–opx offsets are systemically smaller than those predicted by first-principles calculations (Fig. 2). As proposed in Feng et al. (2014), when Ca/Mg is 0.032, 0.067, 0.14, and 1, the $\Delta^{44/40}Ca_{opx-cpx}$ should be 0.37‰, 0.20‰, 0.09‰, and 0.07‰, respectively. In our samples, the highest opx Ca/Mg ratio is 0.019 (H-16) and this has a $\Delta^{44/40}Ca_{opx-cpx}$ of 0.13 ± 0.1‰. While the exact reason for this discrepancy is not known yet, it is possible that the theoretical results may not be fully accurate because the first-principles calculation used an over-simplified chemical composition model which only

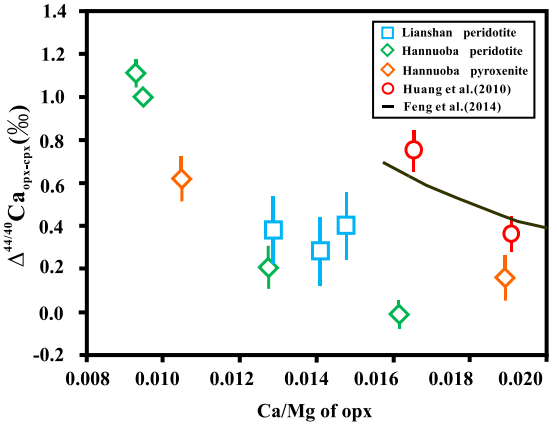

Fig. 2. Variation of $\Delta^{44/40}Ca_{opx-cpx}$ with Ca/Mg (atomic ratio) of opx. CaO contents of opx were calculated by isotope spike method (more details in S-Table 2). The two samples from Huang et al. (2010) are also plotted. Theoretical trend from Feng et al. (2014) is shown as black curve. The error bars of $\Delta^{44/40}Ca_{opx-cpx}$ were calculated by the 2se of cpx and opx from Table 1.

considers the exchange between Ca and Mg. As a major element in opx, Fe may play an important role in changing fractionation factors of Ca isotopes because Ca also substitutes for Fe in opx. Similarly, calculation results of Schauble (2011) also revealed that other elements such as Cr, Co, and Al could affect the force constants of Mg isotopes in spinel.

Ca content in opx is controlled by equilibrium temperature and pressure (Brey and Kohler, 1990), suggesting that equilibrium temperature can affect crystal chemistry and force constant of Ca isotopes in opx at a given pressure. $\Delta^{44/40}Ca_{opx-cpx}$ measured in this study and Huang et al. (2010) are plotted against temperature in Fig. 3. As expected, $\Delta^{44/40}Ca_{opx-cpx}$ of xenoliths in this study is negatively correlated with the Ca-in-opx temperature. And except for P-15, $\Delta^{44/40}Ca_{opx-cpx}$ also depicts a negative trend with the two-pyroxene temperature. The reason for the deviation of P-15 from this trend is not clear. Nevertheless, with equilibrium temperature increasing from 1196 to 1267 K, $\Delta^{44/40}Ca_{opx-cpx}$ decreases dramatically from 1.11‰ to −0.01‰, revealing an unrecognized role of temperature in changing Ca isotope fractionation between opx and cpx, an effect that has not been observed for other isotopes

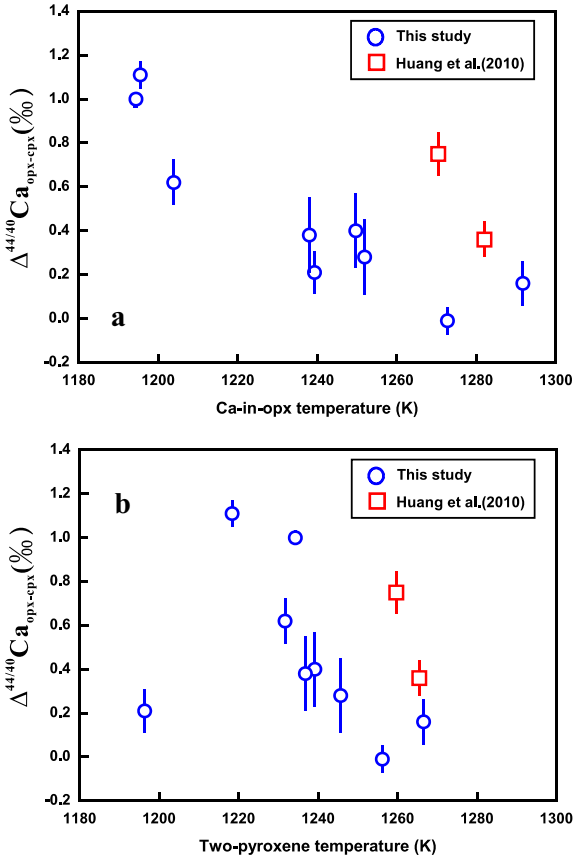

Fig. 3. $\Delta^{44/40}Ca_{opx-cpx}$ of xenoliths in this study show a negative correlation with Ca-in-opx temperatures (a). Except for P-15, $\Delta^{44/40}Ca_{opx-cpx}$ also depicts a negative trend with the two-pyroxene temperature (b). The two samples from Huang et al. (2010) were also plotted. The error bars of $\Delta^{44/40}Ca_{opx-cpx}$ were calculated by the 2se of cpx and opx from Table 1.

like Fe and Mg (e.g., Schauble, 2011; Huang et al., 2013; Young et al., 2015). This can be attributed to the fact that Fe and Mg are major elements in both cpx and opx, and hence temperature variation does not cause resolvable variations on their force constants and isotope fractionation. Our observation suggests that temperature effects on force constants should be taken into account when studying isotope fractionation of minor element systems (e.g., Ca in opx) among minerals.

At a similar Ca/Mg of opx (Fig. 2) and temperature (Fig. 3), the $\Delta^{44/40}Ca_{opx-cpx}$ of San Carlos and Kilborne Hole peridotites from Huang et al. (2010) are significantly larger than the samples from Hannuoba and Lianshan. It is also not clear why there is such discrepancy. It could reflect the large uncertainties of measurement of the low CaO content in opx by electron probe. In our study, we calculated the CaO content of opx based on $^{40}Ca/^{42}Ca$ ratio of sample after spike mixing, i.e., using the isotope spike method (more details can be found in supplementary material S-Table 2). It is also unknown whether kinetic processes may affect the isotopic fractionation in San Carlos and Kilborne Hole samples from Huang et al. (2010). Apparently, more studies on theoretical calculation and measurements for natural samples are needed to better understand Ca isotope fractionation between opx and cpx in San Carlos and Kilborne Hole peridotites.

5.3. Ca isotopic composition in bulk peridotites

Cpx and opx are the two major Ca-bearing minerals in spinel-phase peridotites and pyroxenites. Therefore, Ca isotopic compositions of bulk peridotites and pyroxenites (Table 2) can be estimated based on mineral modes and CaO contents of cpx and opx. The $\delta^{44/40}Ca$ of peridotites and pyroxenites in this study ranges from 0.76‰ to 1.04‰ (Table 2 and Fig. 4), which is comparable to the range (0.96–1.15‰) in previous studies (Amini et al., 2009; Huang et al., 2010; Simon and DePaolo, 2010). Although this range is smaller than the variation of $\delta^{44/40}Ca$ in basalts (up to ~0.7‰) (DePaolo, 2004), it still reveals substantial Ca isotopic heterogeneity in the upper mantle beneath Eastern China. The most primitive sample in our study (LHLS-10) has the highest $\delta^{44/40}Ca$ of 1.04‰ ± 0.12‰, consistent with the average $\delta^{44/40}Ca$ of the upper mantle estimated by Huang et al. (2010) of 1.05 ± 0.04‰. Hereafter, we will discuss the processes responsible for the Ca isotopic variation in peridotites from Eastern China.

5.3.1. Melt extraction process

Amini et al. (2009) observed that $\delta^{44/40}Ca$ is negatively correlated with CaO and positively correlated with MgO in a series of ultramafic rocks. Such correlation can be explained by partial melting of mantle peridotites. Experimental studies on anhydrous melting of peridotites indicated that CaO decreases and MgO increases with progressive melt extraction (Green, 1973). Meanwhile, mantle melting consumes cpx more rapidly than opx in the residue (e.g., Green, 1973; Jaques and Green, 1980). As opx is enriched in heavy Ca isotopes relative to cpx,

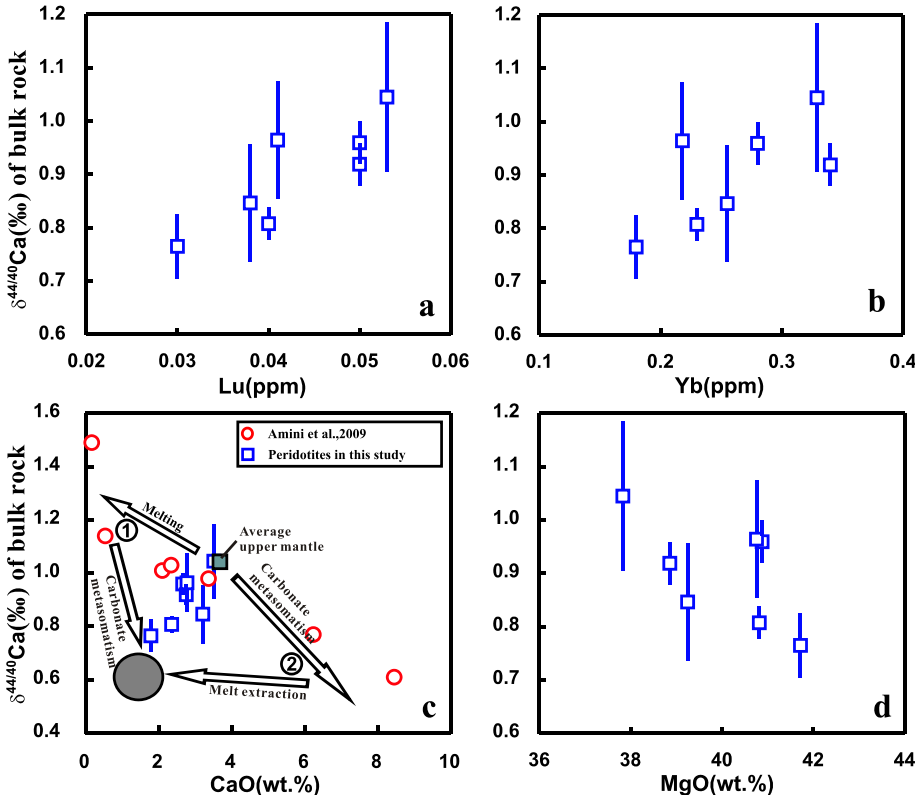

Fig. 4. $\Delta^{44/40}$Ca of whole rock with Lu (a), Yb (b), CaO (c) (including data from Amini et al. (2009)), and MgO (d). $\delta^{44/40}$Ca of whole rocks show positive correlation with elements favoring melt (such as Ca, Y, and Lu) but negative correlation with elements favoring solid residue (like Mg). Process 1: mantle melting followed by subsequent carbonate metasomatism. Process 2: mantle metasomatism followed by subsequent melt extraction. The upper mantle value was from Huang et al. (2010). The error bars of bulk peridotites $\delta^{44/40}$Ca are from Table 2.

the $\delta^{44/40}$Ca of refractory residue should be correlated negatively with CaO and positively with MgO, similar to the observation in Amini et al. (2009). However, on the contrary of the melting trend, $\delta^{44/40}$Ca of 7 spinel lherzolites in this study depict positive correlations with CaO, Yb, and Lu contents, but negatively with MgO content (Fig. 4). Because Ca, Yb, and Lu are preferentially partitioned into melts during mantle melting, the trend of $\delta^{44/40}$Ca with CaO, Yb, Lu, and MgO depicted in peridotites from Eastern China cannot be simply caused by melt extraction of a fertile mantle.

5.3.2. Mantle metasomatism by carbonate melts

Because carbonate sediments in subducted slabs could have higher CaO contents (up to 50 wt.%) and possibly lower $\delta^{44/40}$Ca (−1.09‰ to 1.81‰ with an average value of 0.61‰ from Fantle and Tipper (2014) and references therein) than the primitive mantle with CaO of ~3.65 wt.% (Palme and O'Neill, 2007) and $\delta^{44/40}$Ca of 1.05 ± 0.04‰ (Huang et al., 2010), metasomatism by Ca-rich carbonate melt/aqueous fluids with low $\delta^{44/40}$Ca could easily modify the Ca isotopic composition of the upper mantle. For example, S. Huang et al. (2011) observed that the $\delta^{44/40}$Ca of Hawaiian basalts is correlated with Sr/Nb and $^{87}Sr/^{86}Sr$, which was explained as a result of mixing of recycled ancient marine carbonates and mantle source.

Previous studies on basalts from the NCC revealed metasomatism of carbonates from subducted oceanic crust in their mantle source (Chen et al., 2009; Zeng et al., 2010; Yang et al., 2012; Huang et al., 2015). High U/Pb, Th/Pb, Ce/Pb, and Nb/U ratios in <110 Ma basalts in Yang et al. (2012) relative to the basalts older than 120 Ma reflect recycled oceanic crust features in their mantle source. δ^{26}Mg of <110 Ma basalts ranges from −0.60‰ to −0.42‰, lighter than the normal mantle-derived basalts (−0.24‰, Yang et al., 2012), further suggesting that their mantle source was likely metasomatized by carbonates from the recycled subducted oceanic crust. However, considering that the mantle xenoliths in this study with light Ca isotopic composition also have low Ca and incompatible element contents (Fig. 4) but carbonates usually have high Ca and incompatible element contents, the variation of $\delta^{44/40}$Ca in peridotites cannot be solely explained by carbonate metasomatism. Therefore, we propose a mixing model between a fertile mantle end-member and a depleted one with low $\delta^{44/40}$Ca to explain the trends in Fig. 4. The question focuses on how to form such a mantle reservoir with depleted incompatible element signatures and low

$\delta^{44/40}$Ca. We propose two possible origins for such mantle reservoir:

First, the depleted mantle reservoir could form from melt extraction (which decreased the contents of incompatible elements and increased $\delta^{44/40}$Ca), followed by carbonate metasomatism that lowered the $\delta^{44/40}$Ca and increased CaO content of the peridotites (process 1 in Fig. 4c). However, such process could produce a LREE-enriched pattern in cpx which is contradictory with the LREE-depleted pattern observed in these samples (S-Fig. 2).

Alternatively, it is also possible that the upper mantle was first metasomatized by carbonate and subsequently experienced melt extraction (process 2 in Fig. 4c). Such process can produce a mantle end-member with low Ca content, LREE-depleted pattern, and low $\delta^{44/40}$Ca, more consistent with the geochemical features observed in peridotites in this study.

6. CONCLUSIONS

We measured the co-existing pyroxenes and one olivine from 7 mantle peridotites (4 from North China Craton and 3 from Yangtze Craton) and 2 pyroxenite xenoliths (both from North China Craton) from Eastern China. Ca isotopes are significantly fractionated between co-existing opx and cpx with the $\Delta^{44/40}Ca_{opx-cpx}$ ranging from −0.01‰ to 1.11‰. $\delta^{44/40}$Ca of the ol is 1.16 ± 0.08‰, consistent with the co-existing opx (1.12 ± 0.09‰). We also found that the $\Delta^{44/40}Ca_{opx-cpx}$ is negatively correlated with Ca/Mg (atomic ratio) of opx, which may reflect the compositional effect of Ca content in opx on the inter-mineral fractionation of Ca isotopes. Furthermore, as Ca content of opx is controlled by equilibrium temperature, temperature would also affect the force constants of Ca isotopes in opx, resulting in a negative correlation between equilibrium temperature and $\Delta^{44/40}Ca_{opx-cpx}$. The $\delta^{44/40}$Ca of bulk mantle peridotites estimated based on pyroxene pairs range from 0.76‰ to 1.04‰, revealing considerable Ca isotopic heterogeneity in the upper mantle. The $\delta^{44/40}$Ca values of peridotites from Eastern China show a positive correlation with CaO content and negatively with MgO content, likely due to two end-member mixing between a fertile mantle and a depleted one with low $\delta^{44/40}$Ca which formed by carbonate metasomatism followed by melt extraction.

ACKNOWLEDGEMENTS

This work is financially supported by Natural Science Foundation of China (Nos. 41373007, 41490632, 91328204, 41173031, 41325011, 41090374 and 41090370), the 111 project, the Fundamental Research Funds for the Central Universities. And State Key Laboratory of Isotope Geochemistry grants (SKLIG-KF-12-05, SKLIG-JY-12-01). We thank Gui-Qin Wang, Jin-Long Ma, Ying Liu and Xin Li for help with the analyses. We thank Craig Lundstrom, Roberta Rudnick, Xin-Miao Zhao and Ji-Feng Xu for instructive discussion and Editor Stefan Weyer, Justin I. Simon, Catherine A. Macris and two anonymous reviewers for their helpful and constructive comments.

APPENDIX. A. SUPPLEMENTARY MATERIAL

Supplementary data associated with this article can be found, in the online version, at http://dx.doi.org/10.1016/j.gca.2015.11.039.

REFERENCES

Amini M., Eisenhauer A., Böhm F., Holmden C., Kreissig K., Hauff F. and Jochum K. P. (2009) Calcium isotopes ($\delta^{44/40}$Ca) in MPI-DING reference glasses, USGS rock powders and various rocks: evidence for Ca isotope fractionation in terrestrial silicates. *Geostand. Geoanal. Res.* **33**, 231–247.

Brey G. P. and Kohler T. (1990) Geothermobarometry in four - phase lherzolites II. New thermobarometers, and practical assessment of existing thermobarometers. *J. Petrol.* **31**(6), 1353–1378.

Chen H., Svavage P. S., Valdes M., Puchtel I. S., Day J. M. D., Moreira M., Jackson M., Moynier F. (2014) Heterogeneity of calcium isotope in Earth's mantle. Goldschmidt 2014 Abstracts, 400, California.

Chen L., Tao W., Zhao L. and Zheng T. (2008) Distinct lateral variation of lithospheric thickness in the Northeastern North China Craton. *Earth Planet. Sci. Lett.* **267**, 56–68.

Chen L., Cheng C. and Wei Z. (2009) Seismic evidence for significant lateral variations in lithospheric thickness beneath the central and western North China Craton. *Earth Planet. Sci. Lett.* **286**, 171–183.

De La Rocha C. and DePaolo D. J. (2000) Isotopic evidence for variations in the marine calcium cycle over the Cenozoic. *Science* **289**, 1176–1178.

DePaolo D. J. (2004) Calcium isotopic variations produced by biological, kinetic, radiogenic and nucleosynthetic processes. *Rev. Mineral. Geochem.* **55**, 255–288.

Fantle M. S. and DePaolo D. J. (2007) Ca isotopes in carbonate sediment and pore fluid from ODP Site 807A: the Ca^{2+} (aq) – calcite equilibrium fractionation factor and calcite recrystallization rates in Pleistocene sediments. *Geochim. Cosmochim. Acta* **71**, 2524–2546.

Fantle M. S. and Tipper E. T. (2014) Calcium isotopes in the global biogeochemical Ca cycle: implications for development of a Ca isotope proxy. *Earth Sci. Rev.* **129**, 148–177.

Farkaš J., Buhl D., Blenkinsop J. and Veizer J. (2007) Evolution of the oceanic calcium cycle during the late Mesozoic: evidence from $\delta^{44/40}$Ca of marine skeletal carbonates. *Earth Planet. Sci. Lett.* **253**, 96–111.

Feng C., Qin T., Huang S., Wu Z. and Huang F. (2014) First-principles investigations of equilibrium calcium isotope fractionation between clinopyroxene and Ca-doped orthopyroxene. *Geochim. Cosmochim. Acta* **143**, 132–142.

Green D. H. (1973) Experimental melting studies on a model upper mantle composition at high pressure under water-saturated and water-undersaturated conditions. *Earth Planet. Sci. Lett.* **19**, 37–53.

Griffin W., Andi Z., O'reilly S., Ryan C. (1998) Phanerozoic evolution of the lithosphere beneath the Sino-Korean craton. In *Mantle dynamics and plate interactions in East Asia*, pp. 107–126.

Griffith E. M., Paytan A., Caldeira K., Bullen T. D. and Thomas E. (2008) A dynamic marine calcium cycle during the past 28 million years. *Science* **322**, 1671–1674.

Heuser A. et al. (2002) Measurement of calcium isotopes ($\delta^{44/40}$Ca) using a multicollector TIMS technique. *Int. J. Mass Spectrom.* **220**, 385–397.

Hippler D. et al. (2003) Calcium isotopic composition of various reference materials and seawater. *Geostand. Newslett.* **27**, 13–19.

Huang F., Li S. and Yang W. (2007) Contributions of the lower crust to Mesozoic mantle-derived mafic rocks from the North China Craton: implications for lithospheric thinning. Mesozoic SubContinental Lithospheric Thinning under Eastern Asian. *Geol. Soc. London Spec. Pub.* **280**, 55–75.

Huang F., Zhang Z., Lundstrom C. C. and Zhi X. (2011) Iron and magnesium isotopic compositions of peridotite xenoliths from Eastern China. *Geochim. Cosmochim. Acta* **75**, 3318–3334.

Huang F., Chen L., Wu Z. and Wang W. (2013) First-principles calculations of equilibrium Mg isotope fractionations between garnet, clinopyroxene, orthopyroxene, and olivine: implications for Mg isotope thermometry. *Earth Planet. Sci. Lett.* **367**, 61–70.

Huang S., Farkaš J. and Jacobsen S. B. (2010) Calcium isotopic fractionation between clinopyroxene and orthopyroxene from mantle peridotites. *Earth Planet. Sci. Lett.* **292**, 337–344.

Huang S., Farkaš J. and Jacobsen S. B. (2011) Stable calcium isotopic compositions of Hawaiian shield lavas: evidence for recycling of ancient marine carbonates into the mantle. *Geochim. Cosmochim. Acta* **75**, 4987–4997.

Huang S., Farkaš J., Yu G., Petaev M. I. and Jacobsen S. B. (2012) Calcium isotopic ratios and rare earth element abundances in refractory inclusions from the Allende CV3 chondrite. *Geochim. Cosmochim. Acta* **77**, 252–265.

Huang J., Li S.-G., Xiao Y.-L., Ke S., Li W.-Y. and Tian Y. (2015) Origin of low δ^{26}Mg Cenozoic basalts from South China Block and their geodynamic implications. *Geochim. Cosmochim. Acta* **164**, 298–317.

Jahn B., Auvray B., Cornichet J., Bai Y.-L., Shen Q.-H. and Liu D.-Y. (1987) 3.5 Ga old amphibolites from eastern Hebei Province, China: field occurrence, petrography, Sm–Nd isochron age and REE geochemistry. *Precambr. Res.* **34**, 311–346.

Jaques A. and Green D. (1980) Anhydrous melting of peridotite at 0–15 kb pressure and the genesis of tholeiitic basalts. *Contrib. Mineral. Petrol.* **73**, 287–310.

Kusky T., Li J.-H. and Tucker R. D. (2001) The Archean Dongwanzi ophiolite complex, North China Craton: 2.505-billion-year-old oceanic crust and mantle. *Science* **292**, 1142–1145.

Li S., Xiao Y., Liou D., Chen Y., Ge N., Zhang Z., Sun S.-S., Cong B., Zhang R., Hart S.-R. and Wang S. (1993) Collision of the North China and Yangtse Blocks and formation of coesite-bearing eclogites: timing and processes. *Chem. Geol.* **109**, 89–111.

Liu Y, Zhang Z, Xu J. (2013) Calcium isotope analytical technique for mafic rocks and its applications on constraining the source of Cenozoic ultra-potassic rocks in the Tibetan Plateau. AGU fall meeting abstracts 1, 2627, San Francisco.

Macris C., Manning C. E. and Young E. D. (2015) Crystal chemical constraints on inter-mineral Fe isotope fractionation and implications for Fe isotope disequilibrium in San Carlos mantle xenoliths. *Geochim. Cosmochim. Acta* **154**, 168–185.

Menzies M. A., Xu Y. (1998) Geodynamics of the North China craton. In *Mantle dynamics and plate interactions in East Asia,* pp. 155–165.

Morgan J. L. et al. (2012) Rapidly assessing changes in bone mineral balance using natural stable calcium isotopes. *Proc. Natl. Acad. Sci.* **109**, 9989–9994.

Palme H. and O'Neill H. S. C. (2007) 2.01 – cosmochemical estimates of mantle composition. In *Treatise on Geochemistry* (eds. H. D. Holland and K. K. Turekian). Pergamon, Oxford.

Putirka K. D. (2008) Thermometers and barometers for volcanic systems. *Rev. Mineral. Geochem.* **69**(1), 61–120.

Reisberg L. et al. (2005) Re–Os and S systematics of spinel peridotite xenoliths from east central China: evidence for contrasting effects of melt percolation. *Earth Planet. Sci. Lett.* **239**, 286–308.

Schauble E. A. (2011) First-principles estimates of equilibrium magnesium isotope fractionation in silicate, oxide, carbonate and hexaaquamagnesium (2+) crystals. *Geochim. Cosmochim. Acta* **75**, 844–869.

Simon J. I. and DePaolo D. J. (2010) Stable calcium isotopic composition of meteorites and rocky planets. *Earth Planet. Sci. Lett.* **289**, 457–466.

Skulan J., DePaolo D. J. and Owens T. L. (1997) Biological control of calcium isotopic abundances in the global calcium cycle. *Geochim. Cosmochim. Acta* **61**, 2505–2510.

Tang Y. J., Zhang H. F. and Ying J. F. (2006) Asthenosphere-lithospheric mantle interaction in an extensional regime: implication from the geochemistry of Cenozoic basalts from Taihang Mountains, North China Craton. *Chem. Geol.* **233**, 309–327.

Urey H. C. (1947) The thermodynamic properties of isotopic substances. *J. Chem. Soc.*, 562–581.

Valdes M. C., Moreira M., Foriel J. and Moynier F. (2014) The nature of Earth's building blocks as revealed by calcium isotopes. *Earth Planet. Sci. Lett.* **394**, 135–145.

Wang Y., Zhao Z.-F., Zheng Y.-F. and Zhang J.-J. (2011) Geochemical constraints on the nature of mantle source for Cenozoic continental basalts in east-central China. *Lithos* **125**, 940–955.

Xia Q.-X., Zhi X. C., Meng Q., Zheng L. and Peng Z.-C. (2004) The trace element and Re–Os isotopic geochemistry of mantle-derived peridotite xenoliths from Hannuoba: nature and age of SCLM beneath the area. *Acta Petrol. Sinica* **20**, 1215–1224.

Xu Y.-G., Yu S. and Zheng Y.-F. (2010) Evidence from pyroxenite xenoliths for subducted lower oceanic crust in subcontinental lithospheric mantle. *Geochim. Cosmochim. Acta* **74**, A1164.

Yang W. and Li S. (2008) Geochronology and geochemistry of the Mesozoic volcanic rocks in Western Liaoning: implications for lithospheric thinning of the North China Craton. *Lithos* **102**, 88–117.

Yang W., Teng F.-Z., Zhang H.-F. and Li S.-G. (2012) Magnesium isotopic systematics of continental basalts from the North China craton: Implications for tracing subducted carbonate in the mantle. *Chem. Geol.* **328**, 185–194.

Young E. D., Manning C. E., Schauble E. A., Shahar A., Macris C. A., Lazar C. and Jordan M. (2015) High-temperature equilibrium isotope fractionation of non-traditional stable isotopes: experiments, theory, and applications. *Chem. Geol.* **395**, 176–195.

Zeng G., Chen L.-H., Xu X.-S., Jiang S.-Y. and Hofmann A. W. (2010) Carbonated mantle sources for Cenozoic intra-plate alkaline basalts in Shandong, North China. *Chem. Geol.* **273**, 35–45.

Zhang J.-J., Zheng Y.-F. and Zhao Z.-F. (2009) Geochemical evidence for interaction between oceanic crust and lithospheric mantle in the origin of Cenozoic continental basalts in east-central China. *Lithos* **110**, 305–326.

Zhang S.-B., Zheng Y.-F., Wu Y.-B., Zhao Z.-F., Gao S. and Wu F.-Y. (2006) Zircon U–Pb age and Hf isotope evidence for 3.8 Ga crustal remnant and episodic reworking of Archean crust in South China. *Earth Planet. Sci. Lett.* **252**, 56–71.

Zhang Z.-F., Zhu H.-L., Liu Y., Zhu J.-M., Kang J.-T., Tan D., Liu Y.-F., Wang G.-Q. (2013) A new approach on measuring calcium isotopic compositions using ^{42}Ca–^{43}Ca double spike on Triton-TIMS. AGU fall meeting abstracts 1,2626, San Francisco.

Zhao G., Cawood P. A., Wilde S. A., Sun M. and Lu L. (2000) Metamorphism of basement rocks in the Central Zone of the North China Craton: implications for Paleoproterozoic tectonic evolution. *Precambr. Res.* **103**, 55–88.

Zhu H.-L., Ling M.-X., Zhang Z.-F., Sun W.-D. (2013) Calcium isotopic constraints on the genesis of the Bayan Obo deposit. AGU fall meeting abstracts 1, 2625, San Francisco.

Zhu H.-L., Zhang Z.-F., Liu Y.-F., Liu F., Li X., Sun W.-D., (in press) Calcium isotopic fractionation during ion-exchange column chemistry and thermal ionisation mass spectrometry (TIMS) determination. Geostand. Geoanal. Res.

Zhu P. and Macdougall J. D. (1998) Calcium isotopes in the marine environment and the oceanic calcium cycle. *Geochim. Cosmochim. Acta* **62**, 1691–1698.

Associate editor: Stefan Weyer